

The Dispersion Stability of Colloidal Particles in Dioxane–Water Mixtures

Kazuhiko KANDORI,* Kijiro KON-NO, and Ayao KITAHARA

Department of Industrial Chemistry, Institute of Surface and Colloid Chemistry, Science University
of Tokyo, Kagurazaka 1-3, Shinjuku-ku, Tokyo 162

(Received May 24, 1984)

The dispersion stability of titanium dioxide particles and two kinds of iron(III) oxide particles in dioxane–water mixtures was studied as a function of the dielectric constant ($\epsilon=2.2-78$). The sedimentation of dispersions, the adsorption of sodium 1,2-bis(2-ethylhexyloxycarbonyl)ethanesulfonate (Aerosol OT or AOT) on the particles, and the zeta potential were measured. In the absence of AOT, the dispersions of all the particles were rapidly flocculated over all of the region of the dielectric constant, and little effect of the dielectric constant on the dispersibility was observed. In the presence of AOT, however, the dispersions of all the kinds of particles used were stabilized at both the lower ($\epsilon=2.2$) and higher ($\epsilon=60-78$) regions of the dielectric constant by the adsorption of AOT on the particles. However, the flocculation was accelerated for all kinds of particles, and AOT molecules were not at all, or scarcely, adsorbed on the particles in the middle region of the dielectric constant ($\epsilon=10-50$). This behavior of the dispersibility corresponded with the results of the dynamic light scattering of the AOT solution, which reveal the aggregation of AOT molecules at various dielectric constants. The zeta potential changed from a positive sign to a negative sign with the increase in the dielectric constant, and the isoelectric dielectric point (IED), which means a zero value of the zeta potential, appeared. The order of the values of IED among the three kinds of particles agrees with the order of the isoelectric points (IEP) of the particles. This result can, therefore, be explained by the concept of the acid-base interaction between a particle and a solvent in dioxane–water mixtures.

The theory of the stability of colloidal dispersions in water based on the DLVO theory¹⁾ has been extended to that in nonpolar organic media, and many data on the stability in nonpolar organic media have been accumulated for spherical particles, such as titanium dioxide.²⁻⁷⁾ On the other hand, the dispersion stability of pigments in polar organic media, (e.g., magnetic paints) has recently drawn much attention. The dispersibility of the needle-like particles of iron oxide is very important for magnetic paints. The present authors have previously studied the stability of dispersions of magnetic and nonmagnetic iron(III) oxides and carbon-black particles in 2-butanone as a polar organic medium.⁸⁻¹¹⁾ However, it is difficult to explain the dispersion stability of colloidal particles in several polar organic media, because there are some differences in the characteristics, i.e., the dielectric constant, the solubility parameter, the viscosity, the density, and so on. Lyklema *et al.* have investigated the properties of the electric double layer of the silver iodide particles in a water–ethylene glycol mixture by means of the parameter of the dielectric constant.¹²⁻¹⁴⁾ In their study, the dielectric constant, however, was only varied between 38 and 78, and the dispersion stability in the region of low dielectric constants, especially in nonpolar organic media, was not discussed.

In this paper, the dispersions of two kinds of needle-

like particles of Fe₂O₃-A, B and the spherical particle of TiO₂ for comparison in dioxane–water mixtures were used in order to discuss the effect of AOT as a dispersant. The dielectric constant of dioxane–water mixtures has been reported by Fuoss *et al.*¹⁵⁾ Systems of dioxane–water mixtures have various advantages; for example, water and dioxane mix in all proportions, so that it is possible to connect the aqueous and non-aqueous (nonpolar) systems.

Experimental

Materials. Two kinds of needle-like iron(III) oxides, A and B, and spherical titanium dioxide (Ishihara Sangyo Co., NR, rutile-type) were used. The two kinds of iron(III) oxides A and B, were prepared according to the references.¹⁶⁻¹⁸⁾ The properties of these three samples are shown in Table 1. They were purified by washing with solvents⁸⁻¹¹⁾ and stored in a desiccator before use.

The dioxane used as a solvent was purified and dried from the GR-grade sample as usual and finally treated with Molecular Sieve 4A to remove any trace of water. The deionized water was distilled in Pyrex glass. The conductivity of the water used was less than $1 \times 10^{-6} \text{ mho} \cdot \text{cm}^{-1}$. The AOT used as a dispersant was purified according to an extraction method using a mixture of solvents.¹⁹⁾

Preparation of Dispersions. The dispersions in media of

TABLE 1. PROPERTIES OF THREE KINDS OF PARTICLES

Sample	Class	Shape	Specific surface area (m ² /g)	Axis length or diameter (Å)	Density (g/cm ³)
Fe ₂ O ₃ -A	α -Fe ₂ O ₃	Needle	108	1610×142	3.9
Fe ₂ O ₃ -B	α -Fe ₂ O ₃	Needle	10.3	6770×765	3.9
TiO ₂	Rutile	Spherical	3.1	2330	4.2

various dielectric constants were prepared under ultrasonic irradiation at 20kHz 150 W for 5min. The particle concentration was 0.2wt%. The dielectric constant of the dispersion medium was changed by changing the mixing ratio of dioxane and water.¹⁰

Estimation of Dispersion Stability. The stability of a dispersion was estimated by means of the sedimentation experiment described in previous papers;⁸⁻¹¹ i.e., the sedimentation velocity is the gradient of the time profiles of the sharp boundary between supernatant and sediment.

Measurement of Adsorption of AOT and Zeta Potential.

The amount of adsorption was determined from the measurement of the equilibrium concentrations of AOT in the supernatant with an ultraviolet spectrometer (UV-200S, Shimadzu Co.).¹¹

The zeta potential was measured by microelectrophoresis with the laser Zee TM Model 500 (PEN KEM Co.).⁸⁻¹¹

Measurement of Dynamic Light Scattering. Dust and other extraneous matter were excluded from the solvents through a millipore filter (pore size=0.2μm). The scattered light of each sample solution was measured in a cell which had been rinsed repeatedly with dust-free ethanol. The hydrodynamic radius of a micelle (r_h) was calculated from Einstein-Stokes' equation ($r_h=kT/6\pi\eta D$). The diffusion coefficients (D) for various dielectric constant solutions of AOT were measured by means of a dynamic light-scattering instrument at 30±0.1 °C. The wave length of the Ar laser used was 4880 Å.

Calculation of Potential Energy

The potential energy between particles at various dielectric constants was calculated according to the following equations in order to evaluate the dispersibility of three kinds of particles. The needle-like particles (A and B of Fe₂O₃) used in this study were assumed to be cylindrical, and parallel interaction was considered only for the cylindrical particles, because it is clear that parallel interaction is more predominant than head-tail interaction between the cylindrical particles.^{9,20}

Three kinds of potential energies of the interaction between a pair of particles were considered; steric repulsion between adsorbed layers (V_R^{en}), electrostatic double-layer repulsion (V_R^{el}), and van der Waals attraction (V_A^L or V_A^s). They are expressed in the following equations (1)–(6).

For Needlelike Particles: i) Steric repulsion between adsorbed layers: Here, Ottewill-Walker's equation was utilized:²¹

$$V_R^{en} = \frac{2kTC_v^2}{v_1\rho_2^2} \cdot (\psi_1 - \kappa_1) \cdot V, \quad (1)$$

where V is the total volume of the overlapping zone of the adsorbed layer; C_v , the concentration of AOT in the adsorbed layer; v_1 , the molecular volume of a solvent; ρ_2 , the density of AOT, and ψ_1 and κ_1 the entropic and enthalpic parameters of mixing proposed by Flory.

ii) Electrostatic double-layer repulsion:^{9,20}

$$V_R^{el} = \frac{\epsilon\sqrt{h\kappa}\Psi_0^2}{2\pi} \left[\frac{2}{3} \left(\frac{1}{\exp(\kappa H + 1) + 1} - \frac{1}{\exp(\kappa H) + 1} \right) \right. \\ \times (1 + 3\kappa H) + 2 \left\{ \left(\frac{1}{\exp(\kappa H) + 1} - \frac{1}{\exp(\kappa H + 1) + 1} \right) \kappa H \right. \\ \left. \left. + \frac{1}{\exp(\kappa H) + 1} \right\} + 1.142 \exp(-\kappa H) - 2 \exp(-\kappa H - 1) \right], \quad (2)$$

where h is the radius of the cylinder of a needlelike particle, H is the shortest distance between the particle surface, and κ is the reciprocal Debye length, expressed as follows:

$$\kappa = \sqrt{\frac{8\pi n Z^2 e^2}{\epsilon k T}}. \quad (2)'$$

Equation (2), introduced under an assumption of $\kappa h > 1$ in the previous paper,⁹ was assumed to be useful for the system of the dielectric constant at $\epsilon=2.2$ ($\kappa h < 1$). This assumption is permissible because the contribution of this repulsion is comparatively small in non-polar organic media.²⁰

iii) Van der Waals attraction:¹⁹

$$V_A^L = -\frac{A}{48\pi} \left\{ \frac{1}{(H/2)^2} + \frac{1}{(H/2+h)^2} - \frac{2}{(H/2+h/2)^2} \right\}, \quad (3)$$

where A is the Hamaker constant of the oxide in dioxane-water mixtures. Here, the effect of the adsorbed layer was neglected.

For the Spherical Particle (TiO₂): i) Steric repulsion between adsorbed layers:²¹

$$V_R^{en} = \frac{4\pi kTC_v^2}{3v_1^2\rho_2^2} \cdot (\psi_1 - \kappa_1) \cdot \left(\delta - \frac{H}{2} \right)^2 \cdot \left(3a + 2\delta + \frac{H}{2} \right), \quad (4)$$

where H is the shortest distance between the particle surfaces, a , the radius of a particle, and δ , the thickness of an adsorbed layer.

ii) Electrostatic double-layer repulsion:²²

$$V_R^{el} = \frac{\epsilon a \zeta^2}{2} \ln \{ 1 + \exp(-\kappa H) \}, \quad (5-1)$$

$$V_R^{el} = \frac{\epsilon a^2 \zeta^2}{2a + H} \exp(-\kappa H), \quad (5-2)$$

where ζ is the zeta potential. Eq. (5-1) and Eq. (5-2) were used for the dispersion systems of $\epsilon=10-78$ and $\epsilon=2.2$ respectively.

iii) Van der Waals attraction: Here Vold's equation was used, considering the effect of the adsorbed layer:²³

$$V_A^s = -\frac{1}{12} \left\{ (\sqrt{A_{22}} - \sqrt{A_{33}})^2 \frac{a + \delta}{H} + (\sqrt{A_{33}} - \sqrt{A_{11}})^2 \frac{a}{H + 2\delta} \right. \\ \left. + 4a(\sqrt{A_{22}} - \sqrt{A_{33}})(\sqrt{A_{33}} - \sqrt{A_{11}}) \frac{a + \delta}{(H + \delta)(2a + \delta)} \right\}, \quad (6)$$

where A_{11} , A_{22} , and A_{33} are the Hamaker constants of the TiO₂, a solvent, and the AOT adsorbed respectively.

Results

Effect of AOT on the Stability. In order to examine the effect of the AOT concentration on the dispersibility and the zeta potential, measurements of the sedimentation and zeta potential were carried out in dioxane ($\epsilon=2.2$) and water ($\epsilon=78$) systems for the three kinds of particles. The dependence of the sedimentation velocity and the zeta potential on the AOT concentration for $\text{Fe}_2\text{O}_3\text{-A}$ is shown as an example in Figs. 1(a) and (b). The dispersion stability of both systems is markedly improved by the addition of a small amount of AOT. Similar results were also observed for the $\text{Fe}_2\text{O}_3\text{-B}$ and TiO_2 particles.

The zeta potential showed a maximum in the curves for the dioxane system at the AOT concentration of 3 mM ($1\text{M}=1\text{mol dm}^{-3}$), which approximately coincides with the concentration at which the dispersion stability was attained. On the other hand, it suddenly increased to a constant value upon the addition of a small amount of AOT to the water system.

Effect of Dielectric Constant on the Dispersibility.

In order to examine the effect of the dielectric constant on the dispersibility and the zeta potential, measurements of the sedimentation and the zeta potential were carried out for various dielectric constants for the three kinds of particles. Here, the systems were examined in both the absence and presence of 20 mM AOT. The dependence of the sedimentation velocity and the zeta potential on the dielectric constant is shown as the series of (a) and (b) in Figs. 2, 3, and 4.

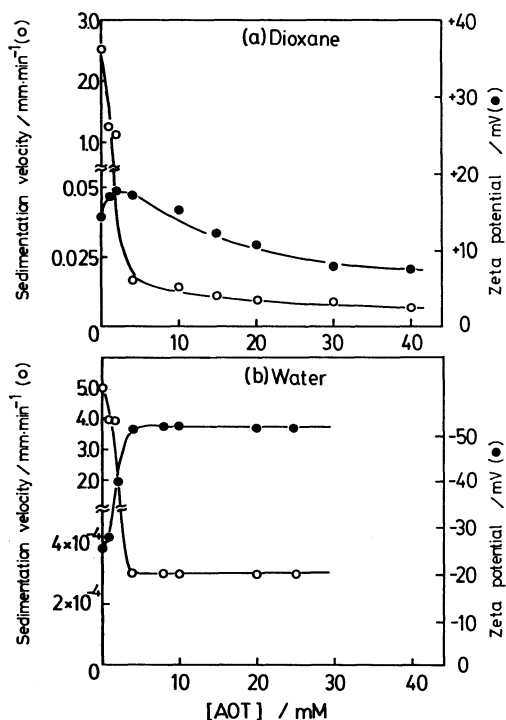


Fig. 1. Plots of the sedimentation velocity and zeta potential *vs.* AOT concentration of $\text{Fe}_2\text{O}_3\text{-A}$ particles for dioxane system(a) and water system(b).

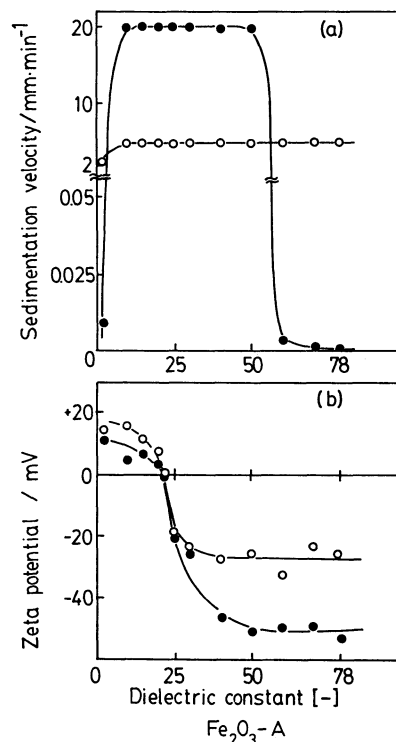


Fig. 2. Change of the sedimentation velocity(a) and zeta potential(b) as a function of the dielectric constant for $\text{Fe}_2\text{O}_3\text{-A}$ particle.

○: In the absence of AOT, ●: In the presence of AOT.

The effect of AOT on the stability of the dispersion is remarkable; the sedimentation velocity is very low in the regions of the lower (at $\epsilon=2.2$) and higher dielectric

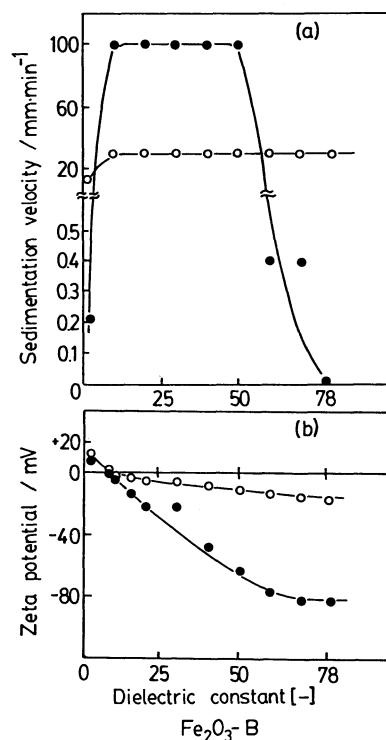


Fig. 3. Change of the sedimentation velocity(a) and zeta potential(b) as a function of the dielectric constant for $\text{Fe}_2\text{O}_3\text{-B}$ particle.

○: In the absence of AOT, ●: In the presence of AOT.

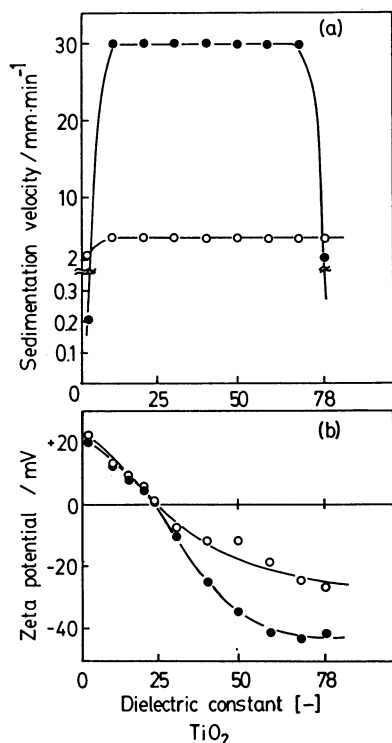


Fig. 4. Change of the sedimentation velocity(a) and zeta potential(b) as a function of the dielectric constant for TiO₂ particle.

O: In the absence of AOT, ●: In the presence of AOT.

constants (at $\epsilon=60-78$), but it suddenly increases in the middle region of the dielectric constants (at $\epsilon=10-50$). This characteristic flocculation of particles in the presence of AOT had previously been observed for carbon-black particles in polar organic media (2-butanone; $\epsilon=15.45$).²⁰ On the other hand, in the absence of AOT, the sedimentation velocity is approximately constant, showing the occurrence of considerable flocculation over all of the regions of dielectric constants for the three kinds of particles.

Figures 2, 3, and 4 show that the value of the zeta potential is inverted from a positive sign to a negative sign with the increase in the dielectric constant and that it converges to the zeta potential of the water system for all of the particles. The absolute value of the zeta potential in the presence of AOT is larger than that in the absence of AOT above the isoelectric dielectric point (abbreviated as IED). The order of the magnitude of IED is as follows:

$$\text{Fe}_2\text{O}_3\text{-B (8)} \ll \text{Fe}_2\text{O}_3\text{-A (22)} < \text{TiO}_2 \text{ (24)}. \quad (\text{A})$$

The figures in brackets show the IED. It is noticeable that the zeta potentials are approximately equal in the neighborhood of the IED for the systems in both the presence and absence of AOT. This result corresponds with the results of the adsorption experiment, which will be shown in Fig. 5.

Effect of Dielectric Constant on Adsorbability of AOT. The adsorption isotherms of AOT for the Fe₂O₃-A particle at various dielectric constants are shown in

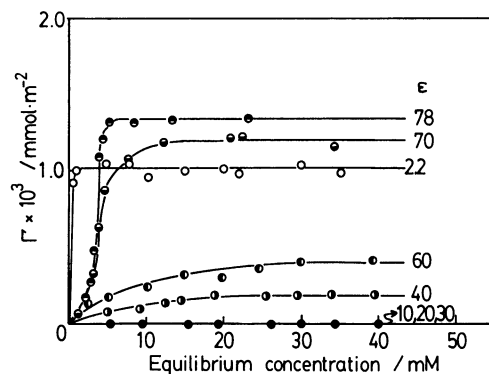


Fig. 5. The adsorption isotherms of AOT for Fe₂O₃-A particle at the various dielectric constants.

TABLE 2. THE DIFFUSION COEFFICIENT (D) MEASURED BY A DYNAMIC LIGHT-SCATTERING METHOD AND THE RESULTING HYDRODYNAMIC DIAMETER (d_h) OF MICELLES AT THE VARIOUS DIELECTRIC CONSTANTS

ϵ (—)	η (cP)	n (—)	$D \times 10^6$ (cm ² /s)	d_h (Å)
2.2	1.087	1.4221	1.83	22.0
10	1.445	1.4060	—	—
20	1.672	1.3926	4.08	6.4
30	1.673	1.3807	5.11	5.2
40	1.538	1.3696	2.06	13.8
50	1.339	1.3595	2.10	15.4
60	1.139	1.3493	2.04	18.8
70	0.945	1.3392	1.62	28.4
78	0.894	1.3300	1.65	29.8

Fig. 5. It is characteristic that AOT molecules are not adsorbed in the region of $\epsilon=10-30$. Furthermore, in the region of $\epsilon=40-60$, the adsorption isotherms are of the Langmuirian type, but their initial slopes are low and the saturation values of adsorption (Γ_m) are smaller than that of $\epsilon=2.2$. On the other hand, in the region of $\epsilon=70-78$, the adsorption isotherms are S-shaped, but the saturation values are higher, belonging to Type I in the Gile-MacEwan-Nakhwa-Smith classification.²⁴ Hence, in the region of $\epsilon=70-78$, the most probable orientation of the first layer is with the nonpolar group outside, while the second layer is adsorbed by interchain cohesion with nonpolar groups and ionic groups outside. This observation agrees with the dispersibility of the particles and the zeta potential as shown in Figs. 2, 3, and 4. The amount of AOT adsorbed on Fe₂O₃-B and TiO₂ could not be measured by the ultraviolet method because of their low specific surface areas.

Effect of Dielectric Constant on Micelle Formation.

The diffusion coefficient (D) and the hydrodynamic diameter of micelles (d_h) at various dielectric constants, as obtained by the dynamic light-scattering method, are listed in Table 2. As may be seen in Table 2, the values of d_h at $\epsilon=2.2$, 70, and 78 are 22, 28.4, and 29.8 Å respectively. Hence, it can be considered that AOT molecules form the reversed micelles at $\epsilon=2.2$ and ordinary micelles at $\epsilon=70$ and 78, because the length of a AOT molecule is approximately 15 Å.

On the other hand, the diffusion coefficient (D)

TABLE 3. NUMERICAL VALUES OF Γ_m , C_v , v_1 AND δ USED FOR Eqs. (1) AND (4)

ϵ (-)	$\Gamma_m \times 10^3$ (mmol/m ²)	C_v (g/cm ³)	v_1 (cm ³)	δ (Å)
2.2	1.02	0.302	1.46×10^{-22}	15
10	0	0	1.26×10^{-22}	0
20	0	0	1.09×10^{-22}	0
30	0	0	9.40×10^{-23}	0
40	0.19	0.056	8.00×10^{-23}	15
60	0.41	0.122	5.40×10^{-23}	15
70	1.20	0.178	4.20×10^{-23}	30
78	1.35	0.200	3.00×10^{-23}	30

could not be measured at $\epsilon=10$, and the values of d_h are very small at $\epsilon=20$ and 30. These facts suggest that AOT molecules do not form micelles, but exist as monomers. The values of d_h are 13.8–18.8 Å in the region of $\epsilon=40$ –60. This suggests that a small part of the AOT molecules associates as dimers or trimers. This change in the aggregation of AOT with the dielectric constant agrees with the results of Elworthy *et al.* for lecithin²⁵ and Kitahara *et al.* for AOT.²⁶

Potential Energies of the Three Kinds of Particles.

The dispersibility of the three kinds of particles at various dielectric constants in the presence of 20 mM of AOT could be evaluated quantitatively from the magnitude of the total potential energy by the use of Eqs. (1)–(6).

The numerical values used for each equation were as follows: In Eqs. (1) and (4), $\psi_1 - \kappa_1 = 0.1$,²⁷ $a = 1165$ Å and $\rho_2 = 1.0$ g/cm³,²⁸ while C_v was calculated from the following equation for each particle: $C_v = \Gamma_m / \delta \cdot S_0$, where δ is the thickness of the adsorbed surfactant molecules and S_0 is the specific surface area of each particle. Γ_m , C_v , v_1 , and δ are listed in Table 3. The amount of AOT adsorbed for Fe₂O₃-B and TiO₂ could not be measured, but it was assumed that the values of Γ_m for the two particles were equal to that for the Fe₂O₃-A particle. In Eqs. (2) and (5), ζ and κ are listed in Table 4. Here, κ was calculated for each particle from Eq. (2)' with the ion concentration (n) obtained from the electric conductivity (k). The values of k and κa and κh are also listed in Table 4. Here, Walden's law was adopted for the system of the solvent mixture.¹⁴ In Eqs. (3) and

(6), the Hamaker constants were as follows. The values of A , 4.6×10^{-20} J, in Eq. (3) for the Fe₂O₃ particle were calculated from the following equation: $A = (\sqrt{A_{11}} - \sqrt{A_{22}})^2$. $A_{11} = 22.6 \times 10^{-20}$ J for the TiO₂ particle,²⁹ $A_{22} = 5.9 \times 10^{-20}$ J for the solvent²⁹ (the values of water and dioxane are equal), and $A_{33} = 2.5 \times 10^{-20}$ J for the adsorbed layer.²⁷

The results of the calculation for the three kinds of particles are shown in Figs. 6, 7, and 8 as the respective potential energy curves respectively. The dispersibility of the three kinds of particles and the effect of the dielectric constant can be discussed quantitatively on the basis of these results.

Discussion

Effect of AOT on the Dispersibility in Dioxane and Water System.

As may be seen in Fig. 1(a) and (b), the dispersion stability of the dioxane and water systems is markedly improved by the addition of a small amount of AOT (4–5 mM). This concentration is of the same order as the critical micellar concentrations of AOT in dioxane and water, which are 5 mM and 5.5 mM respectively.³⁰ Furthermore, at these concentrations of AOT, the adsorption reaches saturation for both systems, as is shown in Fig. 5. This correspondence illustrates the effect of AOT molecules adsorbed on the Fe₂O₃-A particles in both systems.

The appearance of the maximum of the zeta potential in the dioxane system (in the nonpolar system), as is seen in Fig. 1(a), may be explained as follows. At a lower concentration of AOT, the counter ions of the AOT molecules (Na⁺) are preferentially adsorbed on the particle, thus increasing the positive change of the zeta potential, followed by the adsorption of the negative ion (-SO₃⁻), which decreases the zeta potential as the concentration of AOT increases.³¹

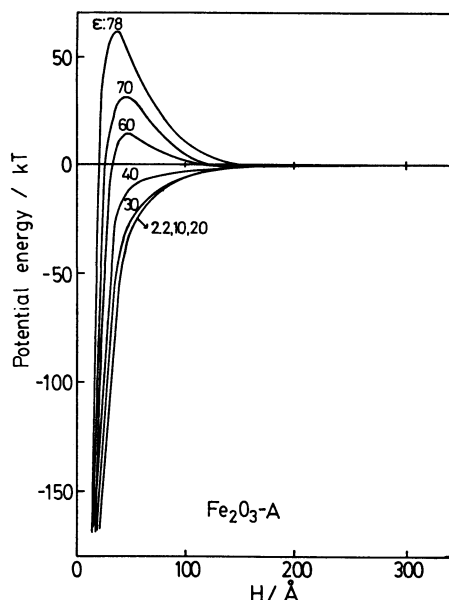
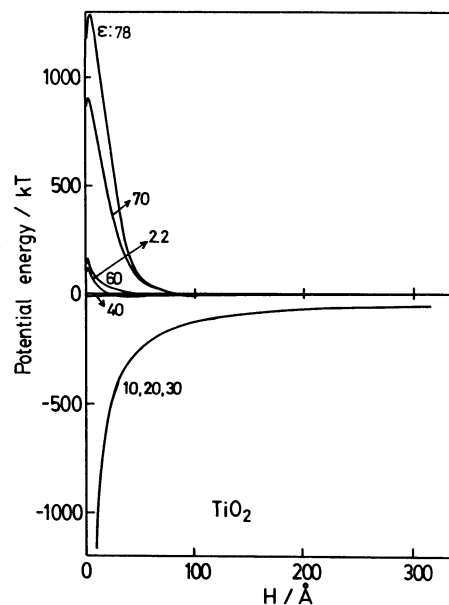
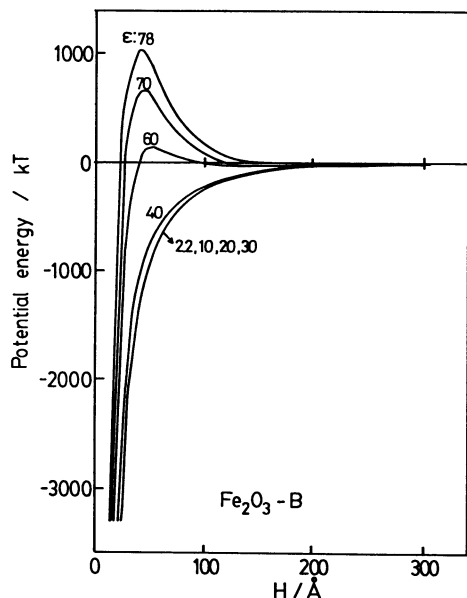
Effect of AOT on the Dispersibility of Three Kinds of Oxides at Various Dielectric Constants.

As may be seen from the series of (a) in Figs. 2, 3, and 4, the effect of AOT is remarkable for all the particles. This fact is correlated with the adsorbability and micelle formation of AOT molecules, as may be seen in Fig. 5

TABLE 4. THE RESULTS OF ζ -POTENTIAL AND κ FOR THE THREE KINDS OF PARTICLES OBTAINED FROM THE ELECTRIC-CONDUCTIVITY METHOD AT VARIOUS DIELECTRIC CONSTANTS (20 mM AOT system)

ϵ	ζ -potential (mV)			k (mho · cm ⁻¹)	κ (cm ⁻¹)	Fe ₂ O ₃ -A	Fe ₂ O ₃ -B	TiO ₂
	Fe ₂ O ₃ -A	Fe ₂ O ₃ -B	TiO ₂			κh^* (-)	κh^* (-)	κa^{**} (-)
2.2	+10.8	+9.8	+20.3	0.05×10^{-6}	1.63×10^5	0.12	0.62	1.90
10	+4.1	-3.7	+9.3	59.8×10^{-6}	2.90×10^6	2.06	11.1	33.7
20	+4.1	-20.4	+4.5	2.87×10^{-4}	4.83×10^6	3.43	18.5	56.3
30	-25.8	-21.0	-10.4	4.26×10^{-4}	4.83×10^6	3.43	18.5	56.3
40	-47.0	-48.3	-25.1	5.31×10^{-4}	4.46×10^6	3.17	17.1	52.0
50	-51.1	-62.6	-34.8	6.30×10^{-4}	4.05×10^6	2.88	15.5	47.2
60	-49.4	-77.8	-41.4	7.60×10^{-4}	3.75×10^6	2.66	14.3	43.7
70	-48.0	-82.5	-43.8	9.20×10^{-1}	3.47×10^6	2.46	13.3	40.4
78	-52.0	-83.6	-41.4	1.090	3.31×10^6	2.35	12.7	38.6

* h : Fe₂O₃-A = 71×10^{-8} cm, Fe₂O₃-B = 382.5×10^{-8} cm. ** a : TiO₂ = 1165×10^{-8} cm.

Fig. 6. Potential energy curves for Fe_2O_3 -A particle.Fig. 8. Potential energy curves for TiO_2 particle.Fig. 7. Potential energy curves for Fe_2O_3 -B particle.

and Table 2. The flocculation of particles in the middle region of the dielectric constants in the presence of AOT is considered to be due to the following reasons. AOT molecules are not at all (at $\epsilon=10-30$) or only a little (at $\epsilon=40, 60$) adsorbed on the particle surface (Fig. 5). Hence, the particles can not be stabilized by the steric repulsion of the adsorbed layer of AOT. Therefore, the counter ion (Na^+) works as an indifferent ion in the middle region of the dielectric constant and the electric double layer is compressed.²⁰ This fact can be seen from κ in Table 4. Therefore, the particles can not be stabilized by the electric double-layer repulsion, either.

As may be seen in Figs. 6, 7, and 8, the potential curves for the three kinds of particles are very similar. That is, in the lower region of the dielectric constants ($\epsilon=2.2-40$), the potential energy is attractive for all

distances, and the maxima of the potential curves do not appear except at $\epsilon=2.2$ for the TiO_2 system. On the other hand, in the region of higher dielectric constants ($\epsilon=60-78$), the maxima of the potential energy (V_{\max}) appear in the potential curves. Moreover, the V_{\max} increases with the increase in the dielectric constant. These results agree with the results of the dispersion stability of the three kinds of particles, as may be seen in Figs. 2, 3, and 4, except that $\epsilon=2.2$ for A and B particles of Fe_2O_3 . Furthermore, these results also agree with the results of the adsorbability and micelle formation of AOT molecules, shown in Fig. 5 and Table 2, except for $\epsilon=2.2$. The exception at $\epsilon=2.2$ is due to the use of Eq. (2) for cylindrical particles at $\epsilon=2.2$, though $\kappa h < 1$, as is shown in Table 4.

Concept of IED. The appearance of IED as seen in Figs. 2, 3, and 4 would be considered on the basis of the concept of acid-base interaction between a particle surface and a solvent as follows. The surface charge is caused by the acid-base interaction between a particle surface and a solvent expressed as Eq. (7):²²



where SH is the surface of a particle and H_2O is either a solvent itself or the water contained in a solvent. If a particle surface is more basic than a solvent, reaction(a) occurs to make the surface positive. In the opposite case, reaction(b) occurs to make the surface negative.

In the region of lower dielectric constants (lower than IED), reaction(a) will occur to make the zeta potential positive, because dioxane is a weakly basic solvent.^{32,33} With the increase in the concentration of water, reaction(a) will shift to reaction(b) to make the zeta potential negative, because water is a strongly basic solvent.³⁴ Hence, the appearance of the IED for all of the particles is considered to result from the shift of

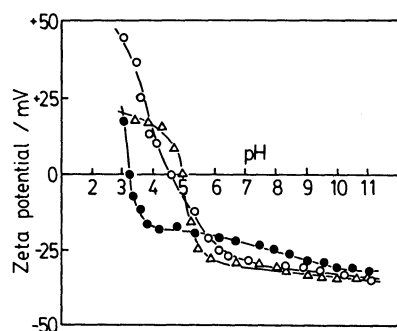


Fig. 9. Change of the zeta potential with pH of the dispersion medium at 20°C.

O: Fe₂O₃-A, ●: Fe₂O₃-B, ▲: TiO₂.

the reaction from (a) to (b).

Comparison of IED for Three Kinds of Particles.

The result of (A) expressing the difference of IED can be explained by the following discussion using the above idea of acid-base interaction. The isoelectric points (IEP) of the three kinds of particles were also measured in order to evaluate the acidity or basicity of each particle. This experiment was done by the measure of the zeta potential under the change in the pH of a dispersion medium by the use of aqueous solutions of 10⁻³ M NaOH and 10⁻³ M HCl. The effect of the ionic strength on the zeta potential was neglected in order to see the zeta potential quantitatively.

The changes in the zeta potential with the pH for the three kinds of particles are shown in Fig. 9. The order of the magnitude of the IEP in Fig. 9 is as follows:

$$\text{Fe}_2\text{O}_3\text{-B (3.2)} < \text{Fe}_2\text{O}_3\text{-A (4.5)} < \text{TiO}_2 \text{ (5.0)}, \quad (\text{B})$$

IEP can be explained by the concept of an acid-base interaction between a particle and a solvent containing the potential-determining ions (H⁺, OH⁻).³⁵ The surface of the Fe₂O₃-B particle is more acidic than that of the Fe₂O₃-A particle. Moreover, the surfaces of Fe₂O₃-A and B are more acidic than TiO₂ particle. This difference is probably due to the conditions of the preparation of the particles and the treatment of the particles.^{36,37}

The order of the magnitude of result (A) agrees very well with result (B). Therefore, the order of IED can be explained by the concept of acid-base interaction between a particle surface and a solvent.

The authors wish to express their thanks to Dr. Kenji Kubota and Professor Yasunori Tominaga, Department of physics, Faculty of Science, Ochanomizu Women's University, for measuring the dynamic light scattering.

References

- 1) E. J. W. Verwey and J. Th. G. Overbeek, "Theory of Stability of Lyophobic Colloids," Elsevier, Amsterdam (1948).
- 2) J. L. van der Minne and P. H. J. Hermanie, *J. Colloid Sci.*, **7**, 600 (1952).
- 3) H. Koelmans and J. Th. G. Overbeek, *Discuss. Faraday Soc.*, **18**, 52, (1954).
- 4) J. L. van der Minne and P. H. J. Hermanie, *J. Colloid Sci.*, **8**, 38 (1953).
- 5) D. N. L. McGown and G. D. Parfitt, *Kolloid Z. Z. Polym.*, **220**, 56 (1967).
- 6) J. Briant and B. Bernelin, *Rev. Inst. France Petrole*, **16**, 1767 (1961).
- 7) D. N. L. McGown and G. D. Parfitt, *J. Colloid Interface Sci.*, **20**, 650 (1965); *Discuss. Faraday Soc.*, **42**, 225 (1966).
- 8) K. Kandori, A. Kitahara, and K. Kon-no, *Bull. Chem. Soc. Jpn.*, **56**, 1581 (1983).
- 9) K. Kandori, K. Kon-no, and A. Kitahara, *Nippon Kagaku Kaishi*, **7**, 963 (1983).
- 10) K. Kandori, A. Kitahara, and K. Kon-no, *J. Colloid Interface Sci.*, **99**, 455 (1984).
- 11) K. Kandori, A. Kazama, K. Kon-no, and A. Kitahara, *Nippon Kagaku Kaishi*, **11**, 1562 (1983).
- 12) J. N. de Wit and J. Lyklema, *J. Electroanal. Chem. Interfacial Electrochem.*, **41**, 259 (1973).
- 13) J. Lyklema and J. N. de Wit, *J. Electroanal. Chem.*, **65**, 443 (1975).
- 14) J. Lyklema and J. N. de Wit, *Colloid & Polymer Sci.*, **256**, 1110 (1978).
- 15) C. A. Kraus and R. M. Fuoss, *J. Am. Chem. Soc.*, **55**, 21 (1933).
- 16) M. Kiyama, *Funtai Oyobi Funmatsu Yakin*, **23**, 177 (1976).
- 17) M. Camras, U. S. Patent 2694656 (1954).
- 18) M. Camras, Kokai Tokyo Koho, 26-7776 (1951).
- 19) A. Kitahara and K. Kon-no, *J. Phys. Chem.*, **70**, 3394 (1966).
- 20) K. Kandori, A. Kazama, K. Kon-no, and A. Kitahara, *Bull. Chem. Soc. Jpn.*, **57**, 1777 (1984).
- 21) R. H. Ottewill and T. Walker, *Kolloid Z. Z. Polym.*, **227**, 108 (1967).
- 22) J. Lyklema, *Adv. Colloid Interface Sci.*, **2**, 65 (1968).
- 23) M. J. Vold, *J. Colloid Sci.*, **16**, 1 (1961).
- 24) C. H. Giles, T. H. McEwan, S. N. Nakhwa, and D. Smith, *J. Chem. Soc.*, 3973 (1960); F. Z. Saleeb, *Kolloid Z. Z. Polym.*, **239**, 602 (1968).
- 25) P. H. Elworthy and D. S. McIntosh, *Kolloid Z. Z. Polym.*, **195**, 27 (1964).
- 26) A. Kitahara, T. Kobayashi, and T. Tachibana, *J. Phys. Chem.*, **66**, 363 (1962).
- 27) D. H. Napper, *Trans. Faraday Soc.*, **64**, 1701 (1968).
- 28) M. Gobe, K. Kon-no, K. Kandori, and A. Kitahara, *J. Colloid Interface Sci.*, **93**, 293 (1983).
- 29) B. Vincent, *J. Colloid Interface Sci.*, **42**, 270 (1973).
- 30) H. B. Klevens, *J. Am. Oil Chem. Soc.*, **30**, 74 (1954).
- 31) A. Kitahara, M. Amano, S. Kawasaki, and K. Kon-no, *Colloid & Polymer Sci.*, **255**, 1118 (1977).
- 32) P. Sorensen, *J. Paint Technology*, **47**, 31 (1975).
- 33) S. Tanaka and T. Satoh, *Shikizai Kyokaishi*, **56**, 753 (1983).
- 34) E. J. Verwey, *Rec. Trav. Chim.*, **60**, 625 (1941).
- 35) K. Tamariuchi and M. L. Smith, *J. Colloid Interface Sci.*, **22**, 404 (1966).
- 36) R. H. Ottewill, and J. M. Tiffany, *J. Oil Colour Chemist Assoc.*, **50**, 844 (1967).
- 37) T. W. Hearly, A. P. Herring, and D. W. Fuestenau, *J. Colloid Interface Sci.*, **21**, 435 (1966).